# Wavelet analysis of an unsteady air-blasted liquid sheet

E. Calvo*, A. Lozano*, O. Nicolis†, M. Marengo†
* LITEC, CSIC-Univ. Zaragoza, María de Luna, 10, 50018 Zaragoza, Spain
† University of Bergamo, Faculty of Engineering, viale Marconi 5, 24044 Dalmine, Italy

**Abstract**

In fluid mechanics wavelet analysis has been often used for modelling and simulation of turbulent flows, since the wavelet methodologies may help in representing the time fluctuations of the power spectra of the turbulent intensity and/or flow velocities. A large aspect ratio air-blasted liquid sheet is very suitable to study the complex mechanisms behind atomization, and in particular, the onset and growth of the instabilities that may lead to the liquid break up. The usual way to define the liquid sheet dynamics is by characterization of the oscillation frequency. This parameter can be determined either measuring the pressure fluctuations near the sheet through a microphone, or recording the obscuration of a laser beam induced by the periodic crossing of the sheet. From the time series of such signals, it is possible to evaluate a typical frequency which is related to the liquid instabilities. Such methods are accurate for stationary conditions of the air-blasted liquid sheets, even if there are experimental evidences that various dynamics regimes may occur, changing the typical frequency for a given water and air velocity. The changes may consist in variations in time and in space, since there are transitions of the power spectra in time for a fixed position and in space for a short time interval, as captured by a high speed camera.

## Introduction

In fluid mechanics wavelet analysis has been often used for modelling and simulation of turbulent flows, since the wavelet methodologies may help in representing the time and space fluctuations of the turbulent flow parameters [1]. Such methods may be applied also to free interface flows, such as liquid sheets and sprays, in order to characterize the regime transitions and give a robust mathematical description of the variation of typical frequencies either in the velocity field or in other dynamical parameters, such as the sheet displacement.

Over the last few years, the large aspect ratio air-blasted liquid sheet has been extensively analyzed to study the complex mechanisms behind atomization, and in particular, the onset and growth of the instabilities that eventually lead to the liquid break up. Although the first studies on liquid sheets initiated at the end of 19th century [2], only starting from 1980 [3,4] researchers are investigating experimentally the complex phenomena of the liquid break-up in large aspect ratio air-blasted configurations. The analysis of instabilities needs a very accurate initial and boundary conditions, and for many studies only a phenomenological analysis is useful [5-7], since the possible discrepancies and the different regimes may be linked with the uncertainties of the nozzle profile, size or of the flow rates. Even if the set-up is well known and the statistical accuracy of the measurements is very high, the liquid sheet oscillations and eventually the break-up, remain difficult to be described in a mathematical way [8]. Both, the power spectra or the time series may represent only a given status in time and space of the liquid sheet, without offering to the researcher a more general scheme to exchange information and to define the kind of transition which eventually occurs.

## Experimental Set-up

The test rig in which the present experiments have been performed has been describe in detail in previous papers [9, 10]. The atomizer head comprising the contoured gas and liquid nozzles, all of them with a span of 80 mm, is connected to the end of a wind tunnel that supplies a properly conditioned airflow. The exit width of the nozzles is 0.4 mm for the liquid sheet, and 3.45 mm for the gas streams. A photograph of the atomizer is displayed in Fig. 1. The water volumetric flow rate, controlled by a rotameter, has extended up to 600 l/h, corresponding to a maximum liquid velocity $U_w$ of 5.2 m/s. The airflow has been varied with a frequency regulator connected to the impulsion fan. The maximum air velocity has been measured to be $U_a$ = 70 m/s.

Two methods have been used to determine the sheet oscillation frequency. In some cases, the acoustic signal generated by the oscillation has been detected using a type 2669 Brüel & Kjaer pressure transducer. Alternatively, the light diffraction method first described by Mansour and Chigier [7] has also been applied. In these measurements, a laser beam is propagated parallel to the liquid sheet, pointing directly to a receiving photodiode. When the oscillating sheet crosses the light beam, it is partially blocked, and a difference in light intensity is detected in the photodiode, resulting in a periodic signal with a frequency related to that of the liquid sheet oscillation. The Fast Fourier Transform (FFT) of the periodic signals has been obtained in a Tektronix TDS3012 oscilloscope equipped with a TDS3FFT module. It has been demonstrated that for all the operating conditions in these experiments both techniques yield almost identical results [11]. The measurements obtained are in very

good agreement with those previously acquired in the same facility [10]. Image sequences have also been recorded with a 512x512 CMOS RedLake HS-4 high-speed camera.

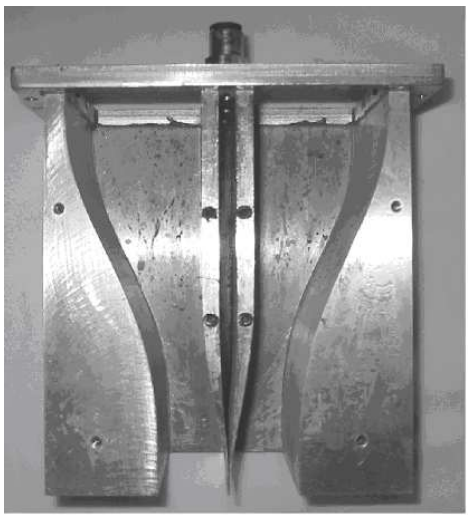

**Figure 1:** View of the nozzle head

**Liquid Sheet oscillation**

Whenever it is subjected to an air co-flow with a velocity higher than a determinate threshold, a liquid sheet oscillates longitudinally usually with a single dominant frequency, although for some conditions a mixture of frequencies can be found. Historically, the sheet visual aspect has served to define different oscillation modes. For example, Stapper and Samuelsen [6] describe a "cellular" break up mode opposed to a "streamwise ligament" one, depending on the presence of either a mesh of perforations, or longitudinal ligaments. Similarly, Mansour and Chigier [5,7] define three zones A, B and C dependent on the gas-liquid relative velocity. According to their description, zone B is characterized by a single dominant sinusoidal mode, and the break up occurs after the appearance of streamwise ligaments, while in zone C the presence of dilatational waves are claimed to prevent the dominant growth of the sinusoidal ones. In zone A, for low water velocities, the break up in longitudinal filaments occurs right at the nozzle lip and no intact sheet length is visible, precluding an accurate frequency measurement.

A recent analysis indicates that in the experimental facility described in the previous Section, more than the three "classical" oscillation regimes can be classified. In particular, 5 different modes have been observed, identified by visual observation and analysis of the FFT spectrum of the periodic microphone or photodiode signals. In some modes a single peak clearly dominates the spectrum, while in others two or even more are present. Transition between modes can be associated to the appearance or disappearance of some of these peaks, or to sudden displacements of the dominant frequency in the case of single peaks. Visually, these changes are normally also reflected in variations in the spray angle, droplet size, or number and shape of liquid ligaments. The following figure, Fig 2, shows two examples of these transitions. Both cases correspond to a same air velocity $U_a$ = 25 m/s. In the first case, the FFT spectrum peak undergoes an abrupt jump to higher values. Although not so visible in the figure, the spray angle narrows. The transition in the second case takes place for higher water velocities, and is also associated to an increase in the oscillation frequency, and a decrease in the spray angle. A more detailed analysis of the different oscillation modes and transitions among them is discussed in Lozano et al. [12].

These transitions present hysteresis, and do not occur for the same water velocity values if they are reached for increasing or decreasing liquid flow rates. In fact, even though in some cases it can be reliably determined when the sheet is oscillating in a specific mode, the transition point is sometimes diffuse. For example, it could be difficult to decide if in a transitional regime, the sheet is alternating between contiguous modes or if it is oscillating in a combination of both. If a signal is recorded for a specific time during which the oscillation regime has been changing, a FFT spectrum of the complete signal will not be capable of providing information of the temporal evolution. An analysis technique capable of preserving a time component, such as the wavelet decomposition, would be very useful in these circumstances.

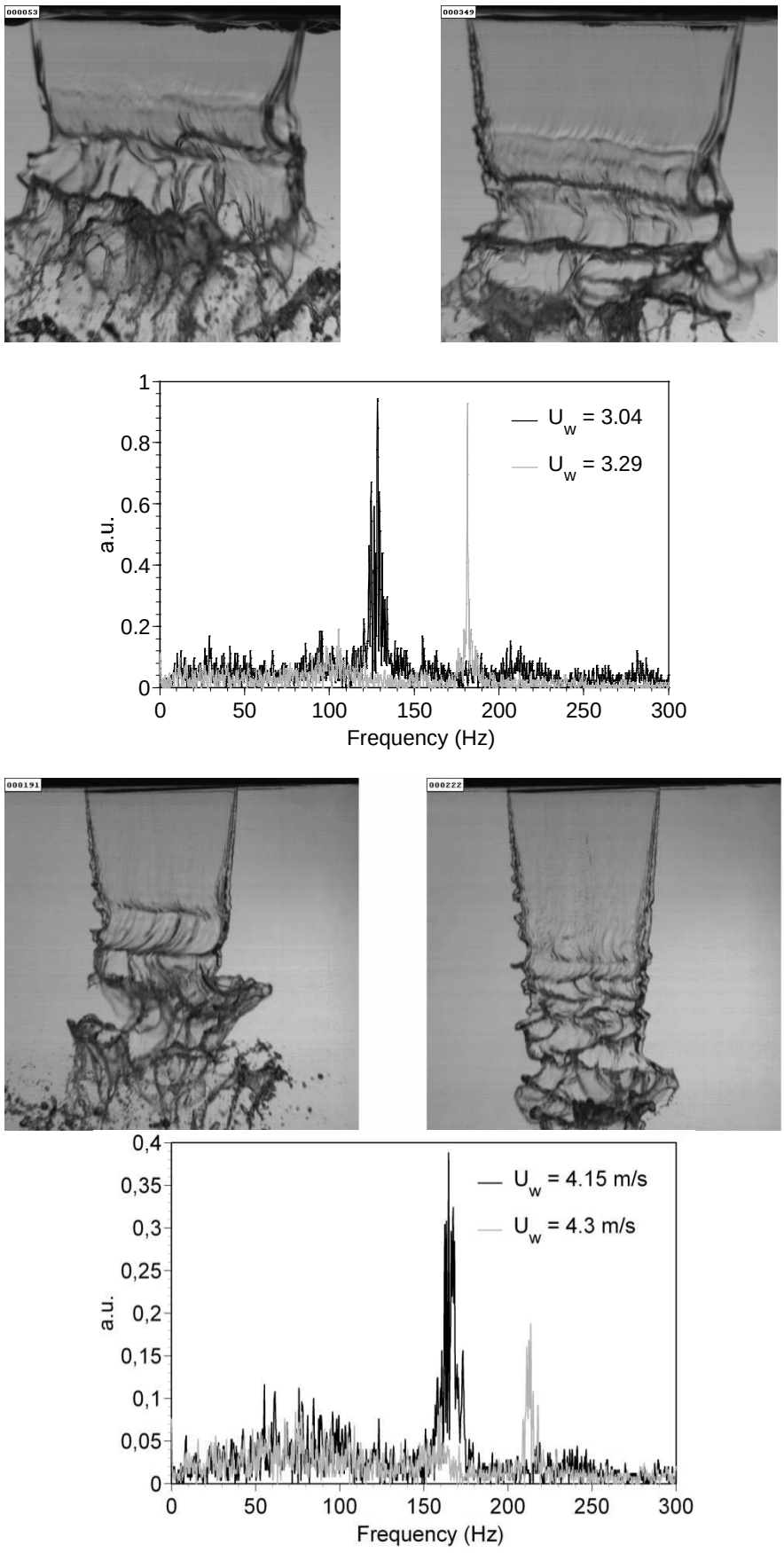


**Fig. 2:** Transitions observed when $U_w$ increases from 3.04 m/s (upper-left) to 3.29 m/s (upper-right), and from 4.15 m/s (lower-left) to 4.3 m/s (lower-right). $U_a$ = 25 m/s

**Wavelet analysis**

Many physical processes are non-stationary and exhibit transient characteristics. Since the Fourier analysis represents the signal by a sum of continuous sinusoids, it is often not suitable for transient data. The Short-Time Fourier Transform (STFT) partially solved this problem by applying the traditional Fourier transform through a fixed-size time window. However, the main downfall of the STFT is its fixed resolution. The width of the windowing function relates to how the signal is represented: a wide window gives better frequency resolution but poor time resolution and a narrower window gives good time resolution but poor frequency resolution (see for example Fig. 3 a) and b)).

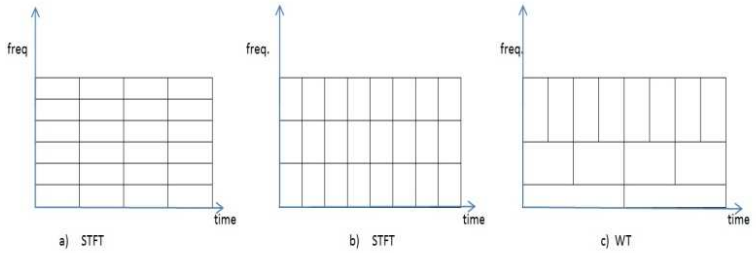


**Fig. 3:** Time frequency decomposition for Short time Fourier transform (a) and (b) and Wavelet transform (c).

The continuous and discrete Wavelet Transform (WT) can be considered an alternative approach to the short time Fourier transform to overcome the resolution problem. In particular, wavelets can be seen as building blocks of wavelet transforms in the same way that the sin and cosines functions are the building blocks of the ordinary Fourier transform. But in contrast to Fourier functions, wavelets can be supported on an arbitrarily small closed interval which allows an adaptive localization in scale (frequency) and in time. The localization property enables to analyze physical situations where the signal contains discontinuities and sharp spikes. Wavelet transform has been recently used for the analysis of non-stationary signals, because it uses short windows at high frequencies and long windows at low frequencies (Fig. 3c). Basics on wavelets and its applications can be found in many texts, monographs, and papers (see for example, Daubechies [12], Vidakovic [13] and Nicolis and Vidakovich [14].

Hence, the wavelet transform is done in a similar way to the STFT in the sense that the signal is multiplied with a function (wavelet) similar to the window function in the STFT, but differently to the STFT the width of the window is changed as the transform is computed for every single spectral component. Unlike the STFT which has a constant resolution at all times and frequencies, the WT has a good time and poor frequency resolution at high frequencies, and good frequency and poor time resolution at low frequencies.

The continuous wavelet transform (CWT) of a function or a signal $x(t) \in L^2(R)$ is defined as

$$X_{CWT}(a,b) = \int_{-\infty}^{\infty} x(t)\psi^*_{a,b}(t)dt\,,$$

where the asterisk denotes complex conjugate and

$$\psi_{a,b}(t) = \frac{1}{\sqrt{|a|}}\psi^*\left(\frac{t-b}{a}\right)$$

is a shifted and scaled version of a characteristic wave-like function $\psi(t)$ known as the "mother wavelet" (a and b represents the shifting and scaling parameters, respectively). The class of wavelet functions is characterized by a finite number of oscillations with fast decay and compact support.

The translation parameter b is related to the location of the window and it is used in the same way as in the STFT. However, in the wavelet transform there is not a frequency parameter, as in STFT, but the “scale parameter” *a* is proportional to *1/frequency*. High scales correspond to a non-detailed global view (low frequency), and low scales correspond to a detailed view (high frequency). In other words, larger scales correspond to dilated signals and small scales correspond to compressed signals.

The frequency value $\omega_a$ of a signal is

$$\omega_a = \frac{\omega_0\,\mathrm{Hz}}{a} \qquad (1)$$

where $\omega_0$ is the fundamental frequency of the wavelet used. For example if we consider the Morlet wavelet (Fig. 4) with an analytical form given by

$$\psi(x) = e^{-x^2/2}\cos(5x)$$

the fundamental frequency is $\omega_0$=0.8.

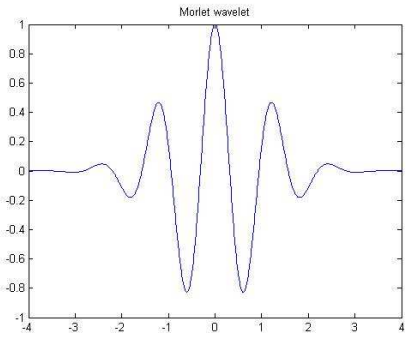


**Fig. 4:** Morlet Wavelet in time domain.

In order to identify the dominant frequency of a signal it is useful to consider the absolute values of wavelet coefficients given by $|X_{CWT}(a,b)|$.

Also, wavelet analysis is a powerful tool for detecting transitions and discontinuity points in time. Consider for example the signal given from the function x(t)=cos(15t) for t in [1, 2.99] and the signal x(t)=sin(4t) for t in [3, 2π], with a data rate of 100Hz for a total of 600 points as shown in Fig. 5 (upper). The time-scale (or time-frequency) representation of the wavelet transform (Fig 5 bottom) allows identifying the discontinuity at point 300 (t=2.99) and the different frequency of the signal before and after this time.

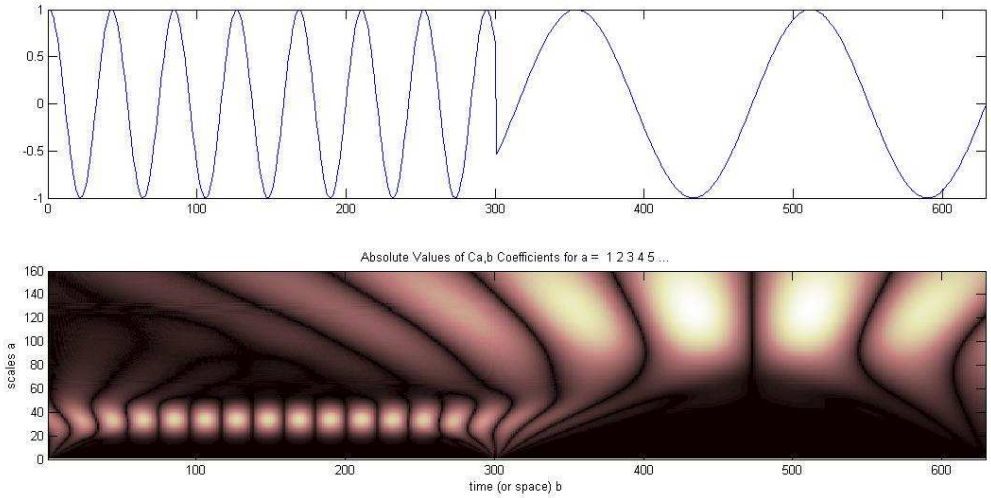


**Fig. 5**: Signal (upper) and absolute values (bottom) of wavelet coefficients using Morlet function

The wavelet analysis in Fig. 5 identify the scales for the lowest and the highest frequencies given by $\omega_1=15/2\pi= 2.3873$ and $\omega_2 =15/2\pi= 0.6366$, respectively. By applying Eq. 1, these frequencies correspond respectively to the scales $a_1=33.5$ and $a_2= 125.6$ in the wavelet domain. Also, wavelet transforms clearly detect the discontinuity at point 300.

**Application**

To illustrate the capabilities of the wavelet analysis to examine time-varying signals, a single data series has been assembled joining together 4 microphone records of 10000 points each, obtained for the same air velocity $U_a$ = 25 m/s and four different water velocities: 2.77 m/s, 2.95 m/s, 3.04 m/s and 3.29 m/s. Each one of these records corresponds to a different typical oscillation frequency, namely 144 Hz, 130.75 Hz, 128 Hz and 181.5 Hz, as derived from the FFT spectra. The frequency reduction when water velocity is continuously increased from 2.77m/s to 3.04 occurs smoothly, without any apparent discontinuity. The jump from 128 Hz to 181.5 Hz between the third and fourth data sets is quite abrupt, and corresponds to the transition depicted in the upper images of Fig. 2. The full data series (40000 points) is shown in the plot of Fig. 6 (data sample rate of 2500Hz).

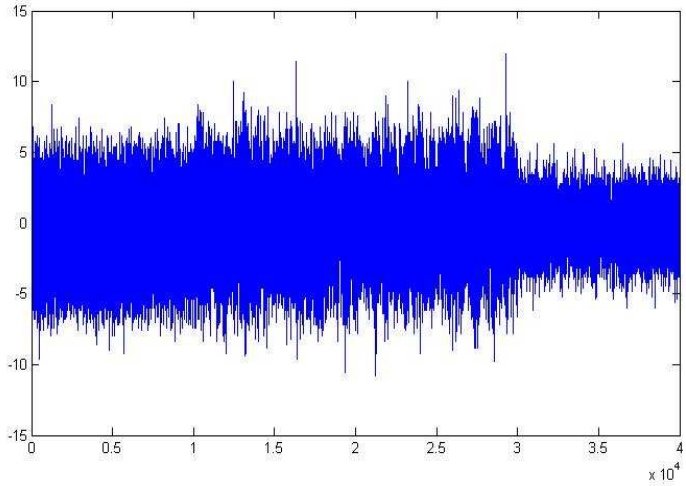


**Fig. 6**: Time series obtained by joining together 4 microphone records of 40000 points (air velocity $U_a$ = 25 m/s and water velocities in a series of 10000 points each: 2.77 m/s, 2.95 m/s, 3.04 m/s and 3.29 m/s).

The CWT allows the identification of the transitions between the four different series. To show this result in a better way we consider the time series nearby the first transitions (from t=9700 to t=10300), as in Fig. 7 (upper). The time-frequency wavelet analysis (Fig. 7 bottom), given by the evaluation of the absolute value of wavelet coefficients at each time *t* and scale *a*, highlights a transition period between time 300 and 360. Instead the scale axis shows a slight frequency decrease after this period (from 150Hz to 130Hz) .

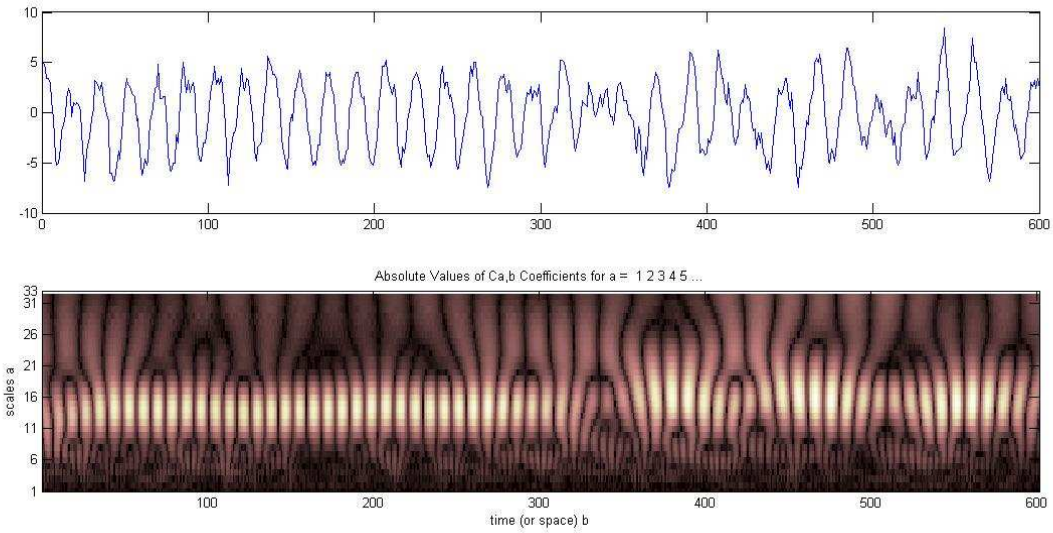


**Fig. 7:** Time series around first transition (upper) and absolute values of Morlet wavelet coefficients (bottom)**.**

Consider now the time series in Fig. 8 (upper) from t=29600 to t=30400. The wavelet analysis (in Fig. 8 bottom) clearly identify a transition around t=400. The wavelet coefficients shows an average frequency around 130 Hz before the transition time. This frequency increases to ~200Hz after the transition time.

**Results and Discussion**

This work represents a first analysis of the liquid instabilities using a methodology widely applied for turbulence, also with interesting results [15]. The wavelet analysis is able in fact to capture the time variation of the signals in terms of a fluctuation of the power spectra, without the compromises of a boxed FFT, due to the difficulty of choosing the right time interval (or window) for the "local" analysis. An advantage of wavelet transforms is that the windows *vary*. In order to isolate signal discontinuities, one would like to have some very short basis functions. At the same time, in order to obtain detailed frequency analysis, one would like to have some very long basis functions. A way to achieve this is to have short high-frequency basis functions and long low-frequency ones. The first goal is to understand if the dynamical transitions and instabilities can be captured by such methodology and if it is possible to describe the fluctuation with few parameters in order to reconstruct the

regime in the most objective way. The present paper considers a first test to use the multilevel wavelet analysis to better understand such unsteady conditions of the liquid sheet. The final goal is in fact to obtain a quantitative tool to define the different dynamical regimes and to compare results from different experimental set-ups.

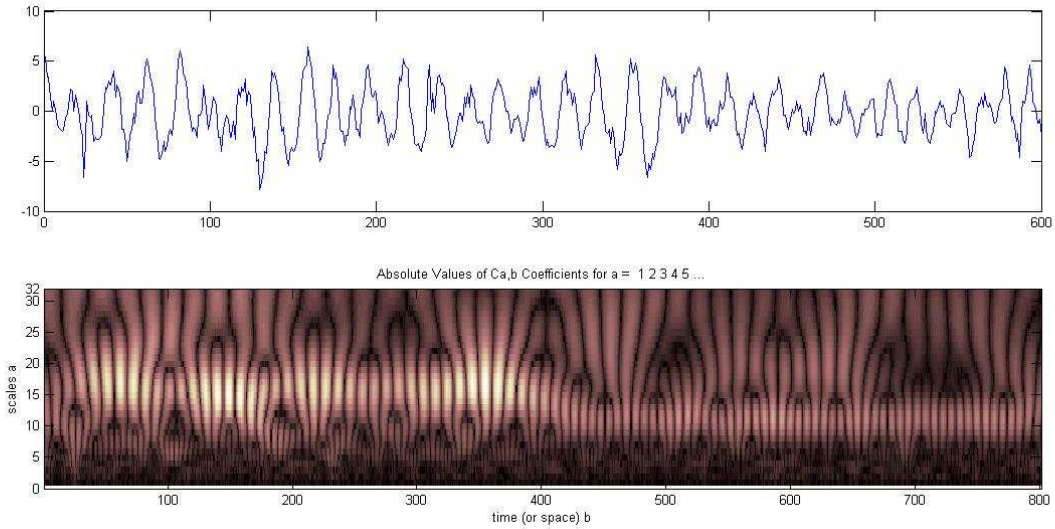


**Fig. 8:** Time series around third transition (upper) and absolute values of Morlet wavelet coefficients (bottom).

**References**

[1] Schneider K., O.V. Vasilyev, Wavelet Methods in Computational Fluid Dynamics, Annual Review of Fluid Mechanics, 42: 473-503

[2] Savart, F., Memoire sur le choc d'une veine liquide lancée contre un plan circulaire, *Ann. de chim.* vol. 54, 56-87 (1833).

[3] Rizk, N.K., and Lefebvre, A.H., The Influence of Liquid Film Thickness on Airblast Atomization, *J. Eng. Power*, vol. 102, 706-710 (1980)

[4] Arai, T. and Hashimoto, H., Disintegration of a Thin Liquid Sheet in a Concurrent Gas Stream, *6th Intl. Conf. on Liquid Atomization and Spray Systems*, London, UK, July 1985.

[5] Mansour, A. and Chigier, N., Disintegration of Liquid Sheets, *Phys. Fluids A*, vol. 2,(5), 706-719, (1990).

[6] Stapper, B. E., Samuelsen, G. S., An Experimental Study of the Breakup of a Two-dimensional Liquid Sheet in the presence of co-flow air shear, *AIAA Paper # 90-0461*, (1990).

[7] Mansour, A. and Chigier, N., (1991), Dynamic Behavior of Liquid Sheets, *Phys. Fluids A*, vol. 3,(12), 2971-2980, (1991).

[8] Sirignano, W.A., and Mehring,C., Review of theory of distortion and disintegration of liquid streams, *Prog. Energy and Comb. Science*, vol. 26, 609-655 (2000).

[9] Lozano, A. Barreras, F., Hauke, G., and Dopazo, C., On the Longitudinal Perturbation of an Air-Blasted Liquid Sheet, *J. of Fluid Mech*., vol. 437, 143-173 (2001).

[10] Lozano, A., Barreras, F., Siegler, C., Löw, D., The effects of sheet thickness on the oscilla-tion of an air-blasted liquid sheet, *Exp. in Fluids*, vol. 39 (1), 127-139, (2005).

[11] Lozano, A., Barreras, F., García, J.A., Calvo, E., Comment on "Experimental investigation on cellular breakup of a planar liquid sheet from an air-blast nozzle", *Phys. Fluids*, 22, 029101 (2010)

[12] Lozano, A., Calvo, E., García, J.A., Barreras, F., Mode Transitions in an Oscillating Liquid Sheet, *ILASS – Europe 2010, 23rd Annual Conference on Liquid Atomization and Spray Systems, Brno, Czech Republic*, September 2010

[13] Daubechies, I., *CBMS-NSF Regional Conference Series in Applied Mathematics 61, SIAM*, Philadelphia (1992).

[14] 13. Vidakovic, B., John Wiley & Sons, New York (1999).

[15] 14. Nicolis, O., and Vidakovic, B. *Current Development in Theory and Applications of Wavelets*. Volume 3, No. 1. (2009)